Application of Z-Source Sparse Matrix Converter for Microturbine Generators

Teymoor Ghanbari
School of Advanced Technologies
Shiraz University
Shiraz, Iran
ghanbarih@shirazu.ac.ir

Amin Farjah, Ehsan Bagheri, Mahdi Raoofat
School of Electrical and Computer Engineering
Shiraz University
Shiraz, Iran
aminfarjah@yahoo.com

***Abstract*— This paper presents a Z-source inverter control strategy for controlling a micro-turbine in autonomous mode. Traditional topologies like back to back PWM converter have some considerable dilemmas such as problems related to usage of bulky DC-link. Matrix converter has been proposed to overcome the problems. But it has some disadvantages such as maximum transfer ratio of 0.86. Here, a z-source sparse matrix converter is proposed to overcome some problems of conventional matrix converter. Reduction of the number of unipolar turn-off power semiconductors, solving the inherent drawback of the low voltage transfer ratio and simple switching strategy are some advantages of the proposed topology. Microturbine dynamic modeling and the proposed converter as well as its controller are introduced in details. A simulation of the overall system is carried out by MATLAB/Simulink. The simulation results show that contrary to matrix converter, the proposed topology can achieve suitable range of voltage transfer ratio and regulates the output voltage in step load variation and disturbance conditions. In addition to mentioned advantages the proposed converter facilitates to employ battery storage for starting up the microturbine and reduce the mutual impact between both sides.**

Keywords—Current controlled mode, Distributed Generation (DG), Microturbine Generation (MTG), Z-source Sparse Matrix Converter (ZSMC)

I. INTRODUCTION

Because of bioenvironmental problems, cost of electricity, transmission loss, freedom in electricity market and several other motivations, the DG units have been more considered over the last decade. The DG sources such as Microturbine Generation (MTG), wind generator, photovoltaic, fuel cell and so on are generally small generation units which are usually connected to distribution networks, near the consumers [1].

Some DGs, for instant MTG, can operate in stand-alone or grid connected modes. Integration of the DG within the existing infrastructure lead to achieve some advantages such as peak shaving, load factor correction, reliability improvement, congestion management and more efficient usage of energy resources. But, there are considerable mutual impacts between the main grid and distribution network in the presence of DGs. Therefore, the control strategy, network stability, protection and many other issues should be studied by accurate system modeling and real time simulation[1-3].

Because MTG is a low noise, low emission and low vibration DG with Combined Heat and Power (CHP) capability, its usage is growing rapidly. MTG uses a high speed turbine (50000 to 120000 rpm) in which the compressor and turbine mounted on the same shaft. In double-shaft MTG, power of the turbine is transferred to a network connected synchronous generator through a gearbox. However, in single-shaft type of MTG a high-speed generation unit, usually a Permanent Magnet Synchronous Machine (PMSM) is mounted on the shaft, and a Power Electronic Interface (PEI) is used to convert the high frequency of the generator to the power frequency of the network [4]. To startup the MTG, the PMSM starts as a motor and drives the microturbine. When the microturbine reaches the suitable speed, the turbine will start to produce the power and the PMSM operates as a generator. The PEI can also handle this function [5, 6].

So far, different PEI topologies such as AC-DC-AC and AC-AC are reported for this application [7-11]. Voltage-Source Converter (VSC) and Current-Source Converter (CSC) are conventional basic converters in the AC-DC-AC topologies. The VSC can only be used for buck DC–AC power conversion or boost AC–DC power rectification, while CSC is applicable as boost DC–AC power conversion or buck AC–DC power rectification[8].

Matrix converter by omitting the DC link capacitor overcomes the DC link problems and is proposed for some different DG interfacing applications, but, it has also some intrinsic restrictions such as low voltage transfer ratio, complexity of switching algorithm and mutual impact of any disturbance of both sides [7, 8]. Other AC-AC converters without the DC link are the matrix converter-based topologies, such as the indirect matrix converter (IMC) [9] and the sparse matrix converter (SMC) [10] as well as the Z-Source AC-AC converter [11].

Here, the Z-Source Matrix Converter (ZSMC) is proposed to connect the MTG to the network, and many advantages of this topology are discussed. The proposed topology solves many problems of both aforementioned converters while takes some advantages of them.

As mentioned earlier, the MTG starts as a motor until it attains a predetermined rotor speed. The proposed topology can fairly provide the required start-up energy from the network, in grid connected mode or by an external storage (such as a battery) in islanded mode. Furthermore, the inverter stage can be used as a common converter for some adjacent sources. In this research the MTG is studied in standalone mode, and a battery is utilized as an external storage.

The next important issue in MTG control is switching strategy. Sinusoidal PWM, space vector PWM and off-line PWM are reported to drive the Machine Side Converter (MSC). The Grid Side Converter (GSC) can be derived by simple modification of the conventional PWMs. Simple constant boost control, SVM based methods; Maximum boost control and Maximum constant boost control are some of the main switching strategies which have been proposed for the Z-source converter [12-14]. Several closed-loop control methods have been reported to achieve a good performance for both the DC-link and the AC output voltage of the ZSI [15].

Shoot-through duty ratio (D0) and modulation index (M) are two independent control variables which can be controlled separately to regulate DC capacitor voltage and AC output voltage, respectively [16]. However, it has been shown that controlling just one of these variables (D0 or M) results in a better regulation of both ac output voltage and DC voltage. Closed-loop control of the peak DC-link voltage has two options as voltage mode (VM) and current mode (CM) control. The CM control has a better response during steady state operation, startup and load step [15].

This paper proposes a ZSMC topology and its controller for a single shaft high speed MTG in islanded mode. Current mode control strategy is implemented based on controlling the control variable D0. The fundamental operation modes of proposed topology are described in details. To evaluate performance of the converter and its controller a load step change and MTG start-up are studied via simulating the system in MATLAB/SIMULINK environment and satisfactory results are achieved.

II. MTG SYSTEM MODELING

The main components of an MTG including compressor, combustor, turbine, recuperator and high frequency generator as well as its PEI and controller are modeled in detail in Fig. 1.

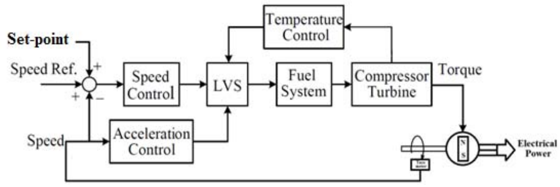

Fig. 1. Block diagram of the MTG

A. Speed, Acceleration and Temperature Control

Fig. 2 shows the block diagram of the speed governor control, acceleration control and temperature controller of the system. In lead-lag transfer function of speed controller, W is the controller gain, X (Y) is the governor lead (lag) time constant, and Z is a constant representing the governor droop or isochronous modes. Using a PI controller, the acceleration is controlled to limit the rate of the rotor speed variation during turbine startup.

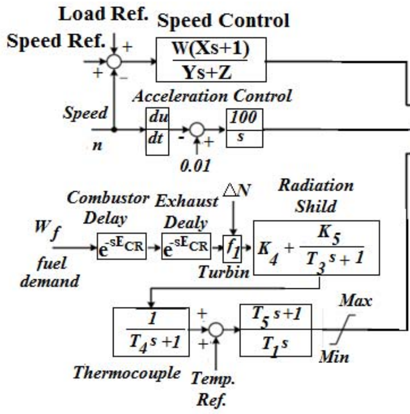

Fig. 2. Speed, acceleration and temperature control block diagram

Temperature controller inputs are fuel flow and turbine speed. The fuel burned in combustor results in turbine torque and exhaust heat. The exhaust temperature characteristic of the single shaft microturbine, f_1, can be calculated by (1).

$$f_1 = T_R + a_{f1}.(1 - W_{f1}) + b_{f2}.\Delta N \qquad (1)$$

where, ΔN is rotor speed deviation and W_{f1} is fuel flow rate. In Fig. 2, K_5 and K_6 are constants of radiation shield transfer function. T_3 and T_4 are the time constants of the radiation shield and thermocouple transfer function, respectively. T_5 and T_t are the time constants of the temperature control transfer function.

B. Fuel system

The main parts of fuel control system are valve positioner and actuator. Equations (2) and (3) are transfer functions of these equipment.

$$E_1 = \frac{a}{bs + c} f_d \qquad (2)$$

$$W_f = \frac{1}{T_f s + 1} E_1 \qquad (3)$$

where, a is the valve positioner gain, b and T_f are the valve positioner and actuator time constant, respectively. W_f is the fuel demand signal in per unit. K_6 is the minimum amount of fuel flow at no-load and rated speed. Fig. 3 shows the fuel system controller.

C. Compressor

The input signals of the gas turbine are the speed deviation and the fuel flow. The output signal is the turbine torque. Dynamic model of the compressor can be expressed by following equation.

$$W_{f2} = \frac{1}{T_{CD} s + 1} W_f \qquad (4)$$

where, T_{CD} is the compressor discharge time constant. The torque characteristic of the single shaft microturbine can be calculated by (5).

$$f_2 = a_{f2} + b_{f2}.W_{f2} + c_{f2}.\Delta N \qquad (5)$$

where, f_2 is a function with inputs of fuel flow and turbine speed. Fig. 4 shows the compressor block diagram. T_{CR} is the combustion reaction time constant and models the delay of the combustor.

D. Permanent Magnet Synchronous Machine (PMSM)

The electric power is generated by high speed PSMG in

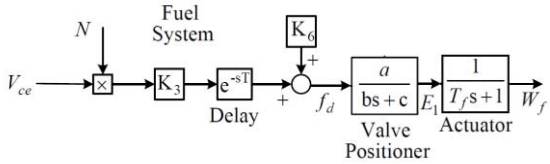

Fig. 3: Fuel system controller block diagram

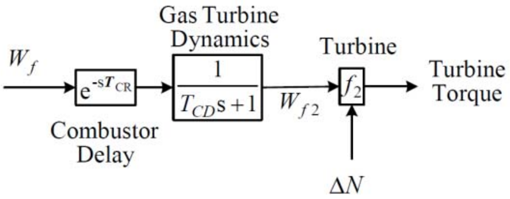

Fig. 4: The compressor block diagram

single shaft MTG. In this paper a 2-pole non salient PMSM is considered. The machine output power is 10 kW and its terminal line to line voltage is 380V. Dynamic model of PMSM including electrical and mechanical equations expressed in the rotor reference frame are as follows:

$$v_d = R_s I_d + L_d \frac{di_d}{dt} - L_q p\omega_r I_q \tag{6}$$

$$v_q = R_s I_q + L_q \frac{di_q}{dt} - L_d p\omega_r I_d + \lambda p\omega_r \tag{7}$$

$$T_e = 1.5p\left[\lambda i_d + (L_q - L_d)i_d i_q\right] \tag{8}$$

$$\frac{d\omega_r}{dt} = \frac{1}{j}\left(T_e - T_{shaft} - F\omega_r\right) \tag{9}$$

$$\omega_r = \frac{d\theta_r}{dt} \tag{10}$$

where L_d and L_q are d-axis, q-axis inductance, respectively, R_s is stator winding resistance, i_d and i_q are d-axis, q-axis current, respectively, v_d and v_q are d-axis, q-axis voltage, respectively, ω_r is angular velocity of rotor, λ is flux linkage, P is number of poles, T_e is electromagnetic torque, J is combined inertia of rotor and load, T_{shaft} is shaft mechanical torque, F is combined viscous friction of rotor and load and θ_r is Rotor angular position.

III. POWER CONVERTER TOPOLOGY FOR MTG

Unlike the split-shaft MTG, single shaft type needs PEI to convert the high frequency AC electric power into power frequency. Power conditioner is a significant component in the single-shaft MTG, and some power conditioner topologies have been presented for this application. One option is three-phase diode rectifier with a voltage source inverter (VSI), but this structure requires an additional inverter for starting the MTG. Back to back PWM converter can rectify this defect and provide bidirectional power flow. Contrary to normal operation, in start-up mode, the machine side converter and the grid side converter operate as inverter and rectifier respectively. Some unconventional converters such as matrix converter have been proposed as PEI in MTG. They can overcome aforementioned inherent limitations of the conventional converters. Some proposed PEI topologies are discussed in following subsections.

The most conventional topology for MTG interface is back to back converter, in which it can be employed a passive or active rectifier in the source side. Some problems such as using an expensive, large, heavy capacitor as the DC-link and considerable energy loss in this DC-link are noticeable drawbacks of back to back converter topology.

To overcome the problems related to the bulky DC-link of back to back converters, matrix converter is proposed in [8] for MTG and in [7] for some other applications. The matrix converter is compact with a high power density. Another good feature of the matrix converter is controllability of the power factor by proper modulation independent of the load type. Low voltage transfer ratio with maximum value of 0.86, complex switching algorithm, large number of unipolar turn-off power semiconductors are some other disadvantages of the matrix converter. In addition, any fluctuation at either side of the converter will directly influence the other side (due to the lack of energy storage). To overcome the low voltage transfer ratio, several solutions based on over-modulation have been reported. But, it can be achieved by expense of low frequency harmonics in both output voltage and input current waveforms. Some structures of matrix converter such as Sparse Matrix Converter (SMC) have simpler switching strategy but utilizing any energy storage is impossible. So, the conventional matrix converter is not yet accepted widely in the industry.

To overcome the inherent limitations of back to back and matrix converters, ZSMC which applies the Z-Source network to the SMC is introduced. Simple modulation strategy, suitable voltage transfer ratio and unity power factor are some advantages of proposed topology. The battery as the secondary power source contributes in start-up, damping the system disturbances and regenerative modes. Fig. 5 shows the proposed ZSMC as the PEI for MTG.

As shown in Fig. 5, the ZSMC has two stages including the rectifier and the inverter stages. An impedance network is provided between the two stages by inductors (L1, L2) and capacitors (C1, C2) that are connected in X shape. Switch S1 is utilized to provide bidirectional power flow [12]. Inductors and capacitors in Z network operate as the energy storage as well as filtering components of the converter.

Fig. 6 shows two different operating modes of the ZSI which is suitable for steady state analysis in order to find the conversion ratio of the ZSI. While, traditional VSIs have 6 active switching vectors {V1:V6} and 2 zero switching vectors {V7:V8}, ZSI increases 7 additional Shoot-Through Zero States (STZS).

For simplification, the Z-source network is supposed to be symmetric with $L1 = L2$ and $C1 = C2$. Therefore, the capacitor and inductor voltages of the Z-source network are:

$$v_{C1}(t) = v_{C2}(t) = v_C(t) \tag{11}$$

$$v_{L1}(t) = v_{L2}(t) = v_L(t) \tag{12}$$

In one of 8 non shoot-through states for an interval of T_1 during switching cycle T, we have:

$$v_L(t) = V_{dc} - v_C(t) \tag{13}$$

$$v_i(t) = v_C(t) - v_L(t)$$

from (13) and (14):

$$v_i(t) = 2v_C(t) - v_{dc} \tag{15}$$

In shoot-through states for an interval of T_{0sh} during T we have:

$$v_L(t) = v_C(t), \quad v_i(t) = 0, \quad T = T_1 + T_{0sh} \tag{16}$$

In the steady state condition, voltage transfer ratio of the converter is calculated by:

$$\overline{v_L(t)} = \frac{1}{T}\int_0^T v_L(t)dt = 0 \tag{17}$$

$$\overline{v_L} = \frac{T_{0sh} \times v_C(t) + T_1 \times (V_{dc} - v_C(t))}{T} \tag{18}$$

$$\frac{V_C}{V_{dc}} = \frac{T_1}{T_1 - T_{0sh}} = \frac{1 - D_0}{1 - 2D_0} \tag{19}$$

where D_0 is shoot-through duty cycle: $D_0 = \frac{T_{0sh}}{T}$

Boost factor can be determined as follows:

$$\hat{v_i}(t) = 2V_C - V_{dc} = \frac{T}{T_1 - T_{0sh}} V_{dc} = BV_{dc} \tag{20}$$

$$B = \frac{1}{1 - 2D_0} \geq 1 \tag{21}$$

where B is the boost factor.

In PWM converter, maximum amplitude of fundamental component of output phase voltage in linear region is:

$$\hat{v}_{ac}(t) = M\frac{\hat{v}_i}{2} = MB\frac{V_{dc}}{2} = G\frac{V_{dc}}{2} \tag{22}$$

where G is Gain factor (or Buck-Boost factor), $G \geq 0$

The number of Z-network operation modes in Z-source converter is more than the conventional type. So, it results in unexpected effects, such as capacitor voltage over-boost [17]. This defect may lead to damage of inverter components, especially when decreasing inductor current becomes equal to half of bridge current. In addition, AC voltage waveform is also distorted in this situation.

In the proposed topology, the battery which is used for starting up the MTG, can also fix the above mentioned problem. In this solution, the battery absorbs any extra energy without serious voltage increasing in the capacitors but a high capacity battery is required.

To calculate elements of the Z network, a symmetrical Z network is assumed. L_1 and L_2 are smoothing inductors and are designed to limit the current ripples to acceptable level of +/- 20% [17] .The inductances can be calculated as:

$$L_1 = L_2 = L = \frac{D_0 V_C}{\Delta I_{max}} \tag{23}$$

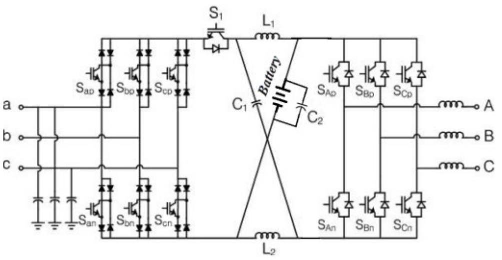

Fig. 5. Proposed ZSMC for MTG application

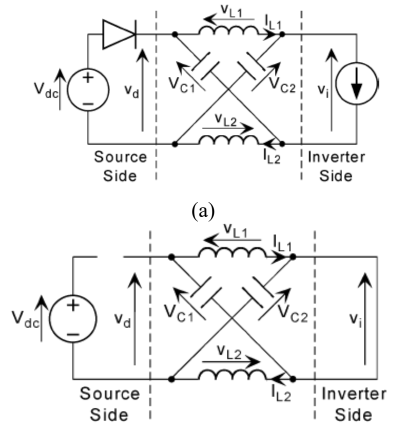

(b)

Fig. 6. Z-source inverter equivalent circuits in a) non shoot-through state. b) shoot-through state [13]

$$\Delta I_{max} = 2I_{Ln} - 2\frac{P_{in}}{V_{DC\,min}} \tag{24}$$

where P_{in} and V_{DCmin} are nominal input power and minimum DC voltage respectively.

Capacitors in the Z-network limit the voltage ripples, while acceptable capacitors voltage ripples are about 1%. Therefore, size of them is determined using:

$$C1 = C2 = C = \frac{D_0 I_{Lav}}{\Delta V_{C\,max}} \tag{25}$$

$$V_{C\,max} = \frac{B+1}{2} V_{DC} \tag{26}$$

where I_{Lav} is the average value of the current of the inductors.

IV. POWER CONVERTER SWITCHING STRATEGY AND CONTROL

Different switching strategies are reported in literature which can be used for this purpose. Here, two suitable methods for Machine Side Converter (MSC) and Grid Side Converter (GSC) are selected to achieve the best performance.

A. Switching strategy

Some PWM methods such as sinusoidal PWM, space vector PWM and off-line PWM can be utilized to drive the MSC. These methods are also modified for driving the ZSI in the grid side. Simple constant boost control, maximum boost control, maximum constant boost control and SVPWM based methods are different modified switching strategies for the ZSI. Simple boost control has the highest voltage stress in a specified gain. Maximum boost control has the lowest voltage stress but it increases volume and cost of the converter, due to the need for larger passive Z-Network. By maximum constant boost control, the inverter will require minimum passive-components, but its harmonics distortion is an important issue. Similar to SVPWM, reduction of output harmonics and more efficient usage of supply voltage are two important advantages of modified SVPWM.

In this paper a modified SVPWM algorithm with a shoot-through capability is utilized for the ZSI in the grid side, and off-line PWM is used as the MSC switching strategy.

Switching sequence of ZSI is shown in Fig. 7. In the modified SVPWM technique, besides the T_1, T_2, and T_0 which are calculated by (27-30), a new shoot-through time interval (T_{0sh}) should be added to the conventional SVPWM in order to boost the DC-link voltage of the ZSI. In shoot-through state, both switches in one leg (i.e. S_{ap} and S_{an}) are turned on simultaneously.

$$T_1 = T \times a \times \frac{\sin(\pi/3 - \alpha)}{\sin(\pi/3)} \quad (27)$$

$$T_1 = T \times a \times \frac{\sin(\alpha)}{\sin(\pi/3)} \quad (28)$$

$$T_0 = T - (T_1 + T_2) \quad (29)$$

$$a = \frac{\left|V_{ref}\right|}{\frac{2}{3}V_{DC}} \quad (30)$$

B. Control strategy

The ZSI system is a non-minimum phase system with a right half plane zero. Therefore, it may be unstable in the case of wide-band feedback loops or feedbacks with high gains. Different control strategies for the MSC have been presented to improve the stability of the ZSI. Generally, GSC regulates the DC voltage and generator speed is controlled by MSC. PQ control strategy is used for grid connected mode and voltage and frequency control strategies are performed in islanding mode.

V. SIMULATION RESULTS

In order to verify the proposed power electronics interface, simulations are carried out using MATLAB/SIMULINK for a 5 KW ZSMC connected the MTG to the grid. More details of the system are tabulated in table I.

TABLE I. THE MTG PARAMETERS

Parameters	Values
Speed governor	Gain=25, X=0.4, Y=0.05, Z=0
Z-network	L1=L2=0.16 mH, C1=C2=500 µF
Battery	6.5-Ah lithium-ion, Vn=200 V
Load	3 kW, 220 V, 50 Hz.
Speed governor	Gain=25, X=0.4, Y=0.05, Z=0
Parameters of PMSG	R = 0.25 Ohms, number of poles p = 2, Ld = Lq = 0.875×10-04 Henrys, λ =0.0534 wb,
Control Parameters	Kp = 5, Ki = 20

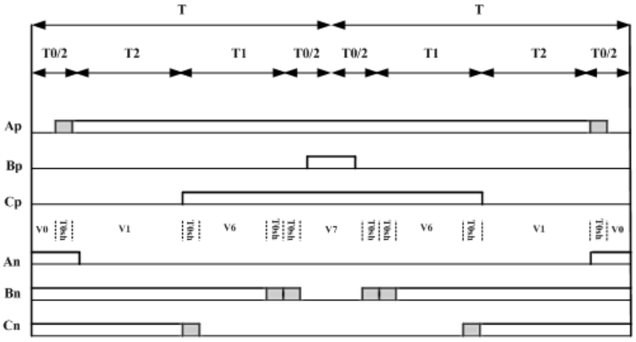

Fig. 7. Modified SVPWM strategy in sixth sector

Fig. 8(a) and (b) show modified SVPWM and off-line PWM signals used as switching strategies for GSC and MSC, respectively.

Fig. 9(a) depicts three-phase output voltage of PMSG in start-up. Fig. 9(b) shows load voltage and current waveforms after the start-up of the MTG using battery storage. The output waveforms verify the suitability of performance of the system using the battery storage. In Fig. 10 the shoot-through time ratio and the line current as well as voltage of the GSC in the case of step load change are shown. The load is increased 0.3 P. U and decreased to its initial value at 3 and 3.5 sec. respectively. As shown in Fig. 10 increasing the shoot-through time ratio by means of current controller in GSC, the output voltage is regulated. Output DC voltage of MSC is shown in Fig. 11.

It should be mentioned that tripled harmonics, especially third order harmonics are very intensive in the output waveforms. They are in phase with each other, so, are not appeared in the line to line voltage. But if there is any single

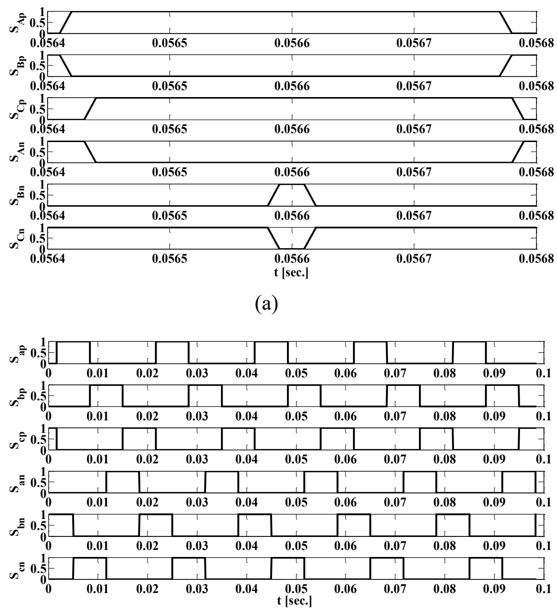

(b)

Fig. 8. a) SVPWM signals for Z-source inverter b) Off-line PWM signals for rectifier stage

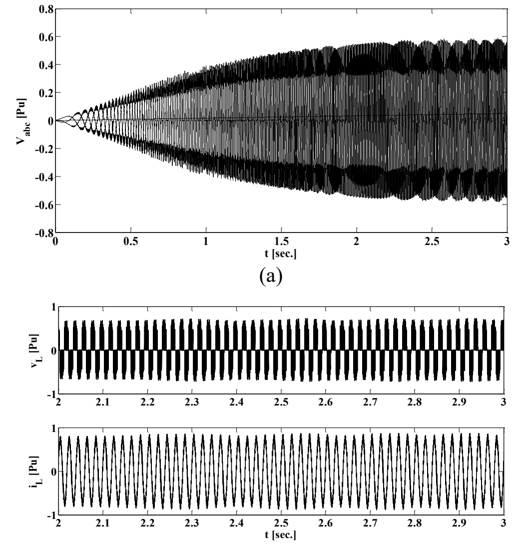

(b)

Fig. 9. MTG start-up, (a) PMSG three-phase voltage (b) Load voltage and current after start-up

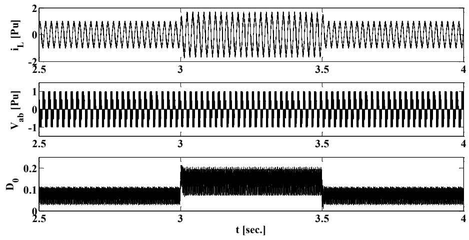

Fig. 10. Step load conditions; output line current, output line voltage and shoot-through time ratio

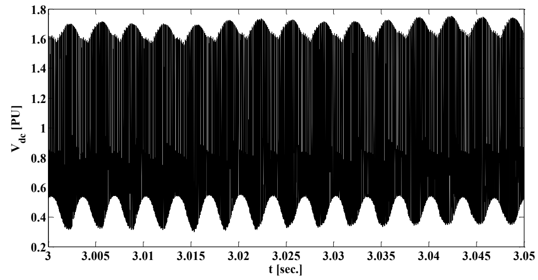

Fig. 11. DC output voltage of rectifier stage affected by third order harmonic

phase load or if the neutral points of three phase loads are grounded, they appear in the phase waveforms.

VI. CONCLUSION

This paper presents a new topology of Z-source Sparse Matrix Converter (ZSMC) for MTG units. The Z-source inverter is very promising for usage in MTG units because of the following unique features and advantages: 1) it is less complex and more cost effective than a back to back or matrix converter, while providing the same functionalities; 2) it has greater reliability, because the shoot-through is not only tolerable but also useful for boosting the voltage, while in back to back and matrix converters topologies, the shoot-through is harmful; 3) in comparison with the matrix converter it has the capability of standalone start-up using a peripheral battery storage. Possible controllers for this converter have reviewed and current controlled mode as a better controller is simulated with satisfactory results.

REFERENCES

[1] "IEEE Application Guide for IEEE Std 1547(TM), IEEE Standard for Interconnecting Distributed Resources with Electric Power Systems," *IEEE Std 1547.2-2008,* pp. 1-217, 2009.

[2] S. Luo, "A review of distributed power systems part I: DC distributed power system," *IEEE Aerospace and Electronic Systems Magazine,* vol. 20, no. 8, pp. 5-16, 2005.

[3] S. Luo and I. Batarseh, "A review of distributed power systems. Part II. High frequency AC distributed power systems," *IEEE Aerospace and Electronic Systems Magazine,* vol. 21, no. 6, pp. 5-14, 2006.

[4] P. Asgharian and R. Noroozian, "Modeling and simulation of microturbine generation system for simultaneous grid-connected/islanding operation," in *Electrical Engineering (ICEE), 2016 24th Iranian Conference on*, 2016, pp. 1528-1533: IEEE.

[5] H. Keshtkar, J. Solanki, and S. K. Solanki, "Dynamic modeling, control and stability analysis of microturbine in a microgrid," in *T&D Conference and Exposition, 2014 IEEE PES*, 2014, pp. 1-9: IEEE.

[6] S. K. Nayak and D. N. Gaonkar, "Modeling and performance analysis of microturbine generation system in grid connected/islanding operation," *International Journal of Renewable Energy Research (IJRER),* vol. 2, no. 4, pp. 750-757, 2012.

[7] T.-D. Mai, G. Van den Broeck, A. Pevere, and J. Driesen, "Power electronics for potential distribution dc power evolution: A review," in *Energy Conference (ENERGYCON), 2016 IEEE International*, 2016, pp. 1-6: IEEE.

[8] S. Chakraborty, B. Kramer, and B. Kroposki, "A review of power electronics interfaces for distributed energy systems towards achieving low-cost modular design," *Renewable and Sustainable Energy Reviews,* vol. 13, no. 9, pp. 2323-2335, 2009.

[9] T. D. Nguyen and H.-H. Lee, "Development of a three-to-five-phase indirect matrix converter with carrier-based PWM based on space-vector modulation analysis," *IEEE Transactions on Industrial Electronics,* vol. 63, no. 1, pp. 13-24, 2016.

[10] J. W. Kolar, F. Schafmeister, S. D. Round, and H. Ertl, "Novel three-phase AC–AC sparse matrix converters," *IEEE Transactions on Power Electronics,* vol. 22, no. 5, pp. 1649-1661, 2007.

[11] F. Z. Peng, "Z-source inverter," *IEEE Transactions on industry applications,* vol. 39, no. 2, pp. 504-510, 2003.

[12] J. Rabkowski, "Improvement of Z-source inverter properties using advanced PWM methods," in *Power Electronics and Applications, 2009. EPE'09. 13th European Conference on*, 2009, pp. 1-9: IEEE.

[13] P. C. Loh, D. M. Vilathgamuwa, Y. S. Lai, G. T. Chua, and Y. Li, "Pulse-width modulation of Z-source inverters," in *Industry Applications Conference, 2004. 39th IAS Annual Meeting. Conference Record of the 2004 IEEE*, 2004, vol. 1: IEEE.

[14] S. Thangaprakash and A. Krishnan, "Modified space vector pulse width modulation for Z-Source inverters," *International Journal of Recent Trends in Engineering,* vol. 2, pp. 136-138, 2009.

[15] M. N. Marwali and A. Keyhani, "Control of distributed generation systems-Part I: Voltages and currents control," *IEEE Transactions on Power Electronics,* vol. 19, no. 6, pp. 1541-1550, 2004.

[16] Y. Li, H. Guo, Q. Xie, and P. Yuan, "Research on the control method for the start of microturbine generation system," in *The 2010 IEEE International Conference on Information and Automation*, 2010, pp. 359-364.

[17] X. Ding, Z. Qian, S. Yang, B. Cui, and F. Peng, "A high-performance Z-source inverter operating with small inductor at wide-range load," in *Applied Power Electronics Conference, APEC 2007-Twenty Second Annual IEEE*, 2007, pp. 615-620: IEEE.